

Theoretical kinetic study of two competing paths in the $\text{H}_2\text{O}_2 + \text{O}(^3\text{P}) \rightarrow \text{HO}_2 + \text{OH}$ reaction

H. Koussa, M. Bahri *

*Laboratoire de Spectroscopie Atomique Moléculaire et Applications, Département de Physique, Faculté des Sciences,
Université Tunis – El Manar, le Belvédère 1060 Tunis, Tunisia*

Received 19 July 2007; received in revised form 10 October 2007; accepted 10 October 2007
Available online 16 October 2007

Abstract

Ab initio-TST calculations were carried out to study the kinetics of the title reaction. The H atom and the OH abstraction paths leading to the same products HO_2 and OH have been considered. The ZPE and BSSE corrected classical barrier heights were predicted to be 7.4 and 17.3 kcal/mol, respectively. Calculated thermal rate constants over the temperature range 300–5000 K showed that the H-abstraction path was the most likely to occur for temperatures below 2500 K which confirms the result found in a previous study [Y. Tarchouna, M. Bahri, N. Jaïdane, Z. Ben Lakdar, J. Mol. Struct. (Theochem), 189 (2003) 664]. The contribution of OH abstraction path to the reaction was predicted to be important for high temperatures.

© 2007 Elsevier B.V. All rights reserved.

Keywords: Hydrogen peroxide; *Ab initio*; TST; Kinetics

1. Introduction

In recent years studies of the hydrogen peroxide reactivity in both gas and aqueous phases have attracted significant attention due to its well established biological and atmospheric interest [1–3]. An instance of this is a theoretical study on the reaction of the H_2O_2 molecule with the oxygen atom $\text{O}(^3\text{P})$ [4] based on the *ab initio*/TST method.



In their study, Bahri et al. [4] considered only the H-abstraction path. Reasonable agreement between modeled and measured rate constants was found indicating that the assumed path is the most probable one for reaction (1) in the considered range of temperature.

This work, using the same *ab initio*/TST method, attempted to investigate the contribution of the OH abstraction path to the same reaction. In the following

the hydrogen abstraction path is pointed to as path1 and the OH abstraction one as path2.

2. Computational methods

All the *ab initio* calculations reported in this communication were performed using the GAMESS program [5] (version R3). Two assumptions were made: (i) path1 and path2 were considered to be independent ones as indicated in Fig. 1. (ii) Each species implied in the reaction via path1 or path2 was taken in the ground state. The stationary structures, the harmonic vibrational frequencies of the reactants, the transition states (TS1 for path1 and TS2 for path2) and the products, the ZPE and the BSSE corrections were performed at the (MCQDPT2//CASSCF) level of calculations as described in [4] with the following improvements: (i) larger active spaces were used for reactants, TS1, TS2 and products. (ii) The Gaussian basis set was extended from cc-pVTZ to aug-cc-pVTZ [6]. For H_2O_2 the active space was of type (6,6); six electrons in six orbitals: the three bonding ($2\sigma_{\text{OH}}$ and one $\sigma_{\text{O-O}}$) orbital

* Corresponding author.

E-mail address: mohamed.bahri2000@yahoo.fr (M. Bahri).

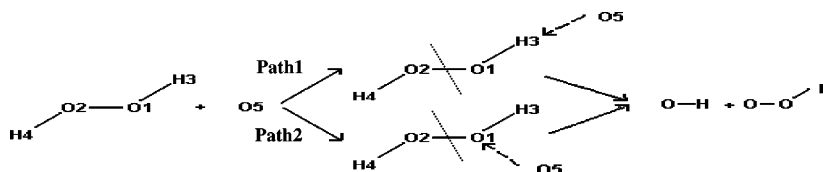


Fig. 1. Assumed mechanism for $\text{H}_2\text{O}_2 + \text{O}$ reaction: hydrogen abstraction path (path1) and OH abstraction one (path2).

and their anti-bonding σ^* ones. For $\text{O}(^3\text{P})$ the active space was of type (4,4); four electrons in four orbitals; the p_x^1 and p_z^1 orbitals of the two unpaired electrons, the doubly occupied orbital p_y^2 and its correlating p_y^* one which have a p_y orbital character.

For TS1 and TS2 the active space contains all the orbitals implied in H_2O_2 and $\text{O}(^3\text{P})$ active spaces.

Two active spaces were considered for each product (OH and HO_2) depending on the considered path. For path1 the active space for OH and HO_2 was of type (5,5) while for path2 it was of type (3,3) for OH and (7,7) for HO_2 .

The results of the electronic structure calculations were used with the transition state theory (TST) as described in [4] to evaluate the rate constant k_1 for path1 and k_2 for path2 over the range of temperature $300 \leq T \leq 5000$ K. The tunneling effect contribution to the reaction was evaluated using the Zero Curvature Tunneling (ZCT) method [7]. Branching ratios τ_1 for path1 and τ_2 for path2 were calculated using the expressions: $\tau_1 = \frac{k_1}{k}$ and $\tau_2 = \frac{k_2}{k} = 1 - \tau_1$, where $k = k_1 + k_2$ is the overall reaction rate constant. All the rate constant calculations were performed by the POLYRATE 8.0 program [8].

3. Results and discussion

Optimized CASSCF geometrical parameters and calculated harmonic vibrational frequencies of the reactants and the products (results not shown) indicated that no sig-

Table 1
Calculated geometrical parameters of TS1 and TS2 activated complexes (bond lengths in Å, angles in degrees)

Parameters ^{a,b}	TS1		TS2
	This work	Ref. [4]	
$R(\text{O1}-\text{O2})$	1.437	1.434	1.919
$R(\text{O1}-\text{H3})$	1.166	1.197	0.971
$R(\text{O2}-\text{H4})$	0.969	0.969	0.972
$R(\text{H3}-\text{O5})$	1.210	1.189	
$R(\text{O1}-\text{O5})$			1.842
$\theta(\text{O2O1H3})$	102.0	102.8	88.9
$\theta(\text{O2O1H4})$	101.0	101.0	90.7
$\theta(\text{O5H3O1})$	178.8	173.2	
$\theta(\text{O5O1O2})$			178.1
$\alpha(\text{H4O2O1H3})$	93.0	93.3	159.4
$\alpha(\text{O2O1H3O5})$	-73.4	-43.4	
$\alpha(\text{O5O1O2H4})$			2.0

^a R, stretch; θ , bending angle; α , torsional angle.

^b See Fig. 2.

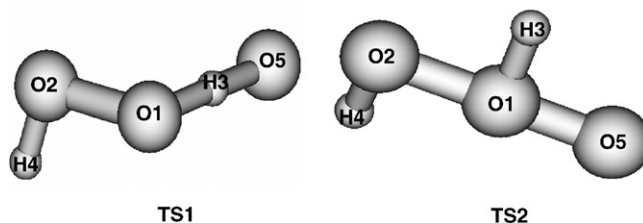


Fig. 2. Geometry of the transition states TS1 for path1 and TS2 for path2.

nificant changes were found compared to those in [4]. The TS1 and TS2 optimized structures are shown in Table 1 and Fig. 2. It can be observed from the TS1 result that the reactive bonds exhibit significant changes with respect of those in [4] when a large active space and extended basis set were used. This improvement moves the transition state on the reaction path toward the reactants and thus can lead to a more reliable description of the exothermic character of the reaction. The predicted values of the (O5H3O1) and (O5O1O2) bending angles were, respectively, 178.8 and 178.1. This may imply that, for both paths, the preferred bringing together of H_2O_2 molecule and O atom for reaction is the one where the reactive atoms (O1, H3, O5 for TS1 and O1, O2, O5 for TS2) are nearly collinear. The calculated Hessian matrix of each activated complex was found to possess only one imaginary frequency, ω^\ddagger which has a magnitude of 3837 cm^{-1} for TS1 and 954 cm^{-1} for TS2. As ω^\ddagger is related to the curvature of the potential energy surface (PES) near the TS, the PES near TS2 is flatter than the one near TS1. The calculated total energies of all species involved in reaction (1) are listed in Table 2. Using these values, the BSSE and/or ZPE corrected MCQDPT2//CASSCF values of the reaction energy and the barrier height were found to be, respectively, 10.5 and 7.4 kcal mol^{-1} for path1 and 10.7 and 17.3 kcal mol^{-1} for path2. The difference between the two calculated reaction energy is considered to be negligible and a unique value of 10.7 kcal mol^{-1} was used in the kinetic calculation. According to these results, it can be assumed that the H-abstraction path compared to the OH abstraction one is the most likely to occur and path2 probably contributes to the reaction (1) only at high temperatures. Therefore kinetics analysis is necessary to examine the contribution of each modeled path to the studied reaction as a function of temperature.

In Table 3, we report the calculated branching ratio and thermal rate constants k_1 and k_2 compared to the experimental ones. Figs. 3 and 4 show the plot of logarithm of

Table 2

Total energies (a.u) of the reactants (H_2O_2 , O), the products (HO_2 and OH) and the activated complexes (TS1 and TS2)

System	CASSCF	MCQDPT2//CASSCF
H_2O_2	−150.943295(16.4) ^a	−151.388302
O	−74.819246	−74.992994
$\text{HO}_2(\text{path1})$	−150.300071(8.7)	−150.738922
$\text{HO}_2(\text{path2})$	−150.323313(8.7)	−150.739807
$\text{OH}(\text{path1})$	−75.468423(5.2)	−75.655061
$\text{OH}(\text{path2})$	−75.440610(5.2)	−75.654586
TS1	−225.718426(12.7)	−226.366725
TS2	−225.719333(14.6)	−226.354024

^a Values in parentheses are the ZPE corrections (kcal/mol).

Table 3

Calculated TST/ZCT rate constants ($\text{cm}^3 \text{ molecule}^{-1} \text{ s}^{-1}$) of reaction (1) compared to experimental values

T (K)	k_1	k_2	Exp. ^a	τ_2
300	2.70(−14)*	6.72(−24)	1.82(−15)	
400	5.60(−14)	9.78(−21)	1.72(−14)	
500	1.13(−13)	9.54(−19)	7.30(−14)	
600	2.18(−13)	2.24(−17)	2.05(−13)	
700	3.93(−13)	2.29(−16)	4.49(−13)	
800	6.65(−13)	1.36(−15)	8.39(−13)	
900	1.06(−12)	5.65(−15)	1.40(−12)	
1000	1.61(−12)	1.80(−14)	2.16(−12)	
1200	3.31(−12)	1.07(−13)	4.34(−12)	
1400	5.96(−12)	4.05(−13)	7.50(−12)	
1600	9.76(−12)	1.13(−12)	1.17(−11)	
1800	1.48(−11)	2.56(−12)	1.70(−11)	
2000	2.13(−11)	5.03(−12)	2.35(−11)	
2200	2.93(−11)	8.88(−12)	3.12(−11)	
2300	3.40(−11)	1.14(−11)	3.54(−11)	
2500	4.43(−11)	1.79(−11)	4.49(−11)	0.30
2800	6.28(−11)	3.18(−11)		0.33
3000	7.72(−11)	4.42(−11)		0.36
3200	9.31(−11)	5.93(−11)		0.39
3400	1.10(−10)	7.73(−11)		0.41
3600	1.29(−10)	9.82(−11)		0.43
3800	1.50(−10)	1.22(−10)		0.45
4000	1.72(−10)	1.50(−10)		0.46
4200	1.96(−10)	1.80(−10)		0.48
4400	2.21(−10)	2.14(−10)		0.49
4600	2.48(−10)	2.52(−10)		0.50
4800	2.76(−10)	2.92(−10)		0.51
5000	3.06(−10)	3.36(−10)		0.52

* Power of 10 in parentheses.

^a Ref. [9].

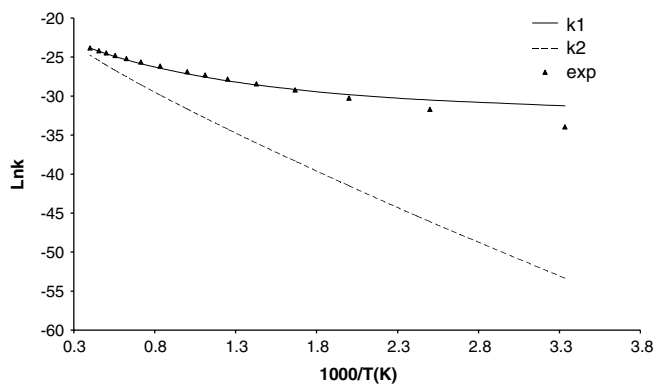


Fig. 3. Plot of logarithm of the modeled rate constants ($\text{cm}^3 \text{ molecule}^{-1} \text{ s}^{-1}$) versus $1000/T$ (K) compared to the experimental result.

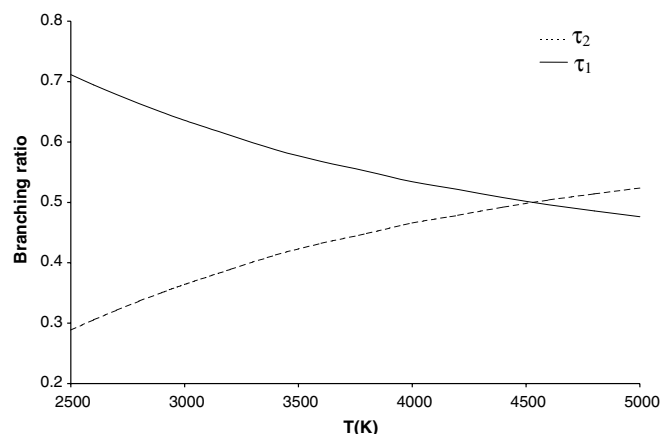


Fig. 4. Plot of the branching ratios versus T (K).

k_1 and k_2 versus $1000/T$ (K) and the plot of the branching ratios τ_1 and τ_2 versus T (K), respectively. It can be noted that the modeled rate constants k_1 were in reasonable agreement with the experimental result for temperature ranging from 300 to 2500 K. In this range of temperature the modeled rate constants k_2 underestimate the experimental ones. This can be interpreted as follows: in the considered range of temperature, the major contribution to reaction (1) comes from the H-abstraction path. Hence it can be said that this path is the most probable which confirms previous finding [4]. At higher temperatures, where no experimental results are available, the calculated branching ratio τ_2 would increase from 0.3 at 2500 K to 0.5 at 4500 K. Our calculations predict that the contribution of the path2 to the title reaction becomes important at high temperatures. This remains to be validated by high temperature measurement of the rate constant of the reaction.

Acknowledgements

The authors are grateful to Prof. Donald G. Truhlar, Department of Chemistry University of Minnesota, for the license access to POLYRATE program.

We are also grateful to Mr. Ayadi Hajji from the Engineering School of Sfax for his help with English.

References

- [1] A.M. Pimenta, S.H.F. Scafi, C. Pasquini, I.M. Raimundo Jr., J.J.R. Rohwedder, M. da C.B.S.M. Montenegro, A.N. Araujo, J. Near Infrared Spectrosc. 11 (2003) 49.
- [2] H. Voraberger, V. Ribitsch, M. Janotta, B. Mizaikoff, Appl. Spectrosc. 57 (2003) 574.
- [3] Davide Vione, Valter Maurino, Claudio Minero, Ezio Pelizzetti, Ann. Chim. 93 (2003).
- [4] Y. Tarchouna, M. Bahri, N. Jaïdane, Z. Ben Lakdar, J. Mol. Struct. (Theochem) 189 (2003) 664.
- [5] M.W. Schmidt, K.K. Baldrige, J.A. Boatz, S.T. Elbert, M.S. Gordon, J.H. Jensen, S. Koseki, N. Matsunaga, K.A. Nguyen, S.J. Su, T.L. Windus, M. Dupuis, J.A. Montgomery, J. Comput. Chem. 14 (1993) 1347.

- [6] T.H. Dunning Jr., J. Chem. Phys. 90 (1989) 1007.
- [7] A. Gonzalez-Lafont, T.N. Truong, D.G. Truhlar, J. Chem. Phys. 95 (1991) 8875.
- [8] R. Steckler, Y.Y. Chuang, P.L. Fast, E.L. Coitino, J.C. Corchado, W.P. Hu, Y.P. Liu, G.C. Lynch, K.A. Nguyen, C.F. Jackels, M.Z. Gu, I. Rossi, S. Clayton, V.S. Mellissas, B.C. Garrett, A.D. Issacson, D.G. Truhlar, POLYRATE-version 7.3.1, University of Minnesota, Minneapolis, 1997.
- [9] NIST Chemical Kinetic Database, Available from: <<http://kinetics.nist.gov/kinetics/>>.